



# Polycaprolactone–carboxymethyl cellulose composites for manufacturing porous scaffolds by material extrusion

M. E. Alemán-Domínguez<sup>1</sup>  Z. Ortega<sup>1</sup>  A. N. Benítez<sup>1</sup> Mario Monzón<sup>2</sup> L. V. Garzón<sup>1</sup> Sara Ajami<sup>3</sup> Chaozong Liu<sup>3</sup>

<sup>1</sup> Departamento de Ingeniería de Procesos, Universidad de Las Palmas de Gran Canaria, Edificio de Fabricación integrada, Parque Científico-Tecnológico de la ULPGC, 35017 Las Palmas, Spain

<sup>2</sup> Departamento de Ingeniería Mecánica, Universidad de Las Palmas de Gran Canaria, Edificio de Fabricación integrada, Parque Científico-Tecnológico de la ULPGC, 35017 Las Palmas, Spain

<sup>3</sup> Institute of Orthopaedic and Musculoskeletal Science, Royal National Orthopaedic Hospital, University College London, Stanmore, London HA7 4LP, UK

**B** M. E. Alemán-Domínguez mariaelena.aleman@ulpgc.es

## Abstract

Polycaprolactone–carboxymethyl cellulose<sup>1</sup> composites have been obtained and used to print porous structures by material extrusion. The materials used contained 0, 2 and 5% w/w of the carboxymethyl cellulose additive. These structures have been analyzed in terms of their morphology (including the evaluation of their porosity), mechanical properties under compression load and cell affinity. Cell affinity has been evaluated by culturing sheep mesenchymal stem cells and analyzing their viability by the Alamar Blue<sup>®</sup> assay at days 1, 3, 6 and 8. The results show that composites samples have similar values of porosity and apparent density than pure polycaprolactone ones. However, samples containing 5% w/w of carboxymethyl cellulose have micropores on the filaments due to a hindered deposition process. This characteristic affects the mechanical properties of the structures, so these ones have a mean compression modulus significantly lower than pure polycaprolactone scaffolds. However, the samples containing 2% w/w of carboxymethyl cellulose show no significant difference with the pure polycaprolactone ones in terms of their mechanical properties. Moreover, the presence of 2% w/w of additive improves cell proliferation on the surface of the porous structures. As complementary information, the flow properties of the composite materials were studied and the power law equations at 210 °C obtained, as this temperature was the 3D printing temperature. These equations can be useful for simulation and designing purposes of other manufacturing processes.

**Keywords** Additive manufacturing · Tissue engineering · Viscosity model · Biomaterials · 3D printing · Bone regeneration

## Introduction

Polycaprolactone (PCL) is a polymeric biomaterial used in tissue engineering applications because of its biocompatibility, ease to process and slow degradation rate [1]. There is a large experience about the processing of the material by additive manufacturing techniques, in particular under the process category of “material extrusion (ISO/ASTM 52900:2015)”, commonly known as fused deposition modeling (FDM) [2, 3]. Other processes are based on the deposition of a solution of this polymer in an appropriate solvent, such as acetic acid [4]. Nevertheless, the hydrophobicity of this polymer limits its wettability and cell attachment [1, 5, 6]. This characteristic is a clear disadvantage for the manufacturing of scaffolds intended to be used as support material for the regeneration of bone.

To overcome this limitation, there is a trend to develop new composite biomaterials for additive manufacturing, like the combination of PCL with bioactive glass [7], tricalcium phosphate [8, 9] or hydroxyapatite [10].

Regarding the introduction of organic additives, authors of this paper have demonstrated in previous work [11] that microcrystalline cellulose can be used as a filler of polycaprolactone matrices with a positive effect both on the mechanical properties and the bioaffinity of the scaffolds 3D printed with these composite materials. In this study, carboxymethyl cellulose (CMC) has been proposed as an additive expected to have similar

results than cellulose. CMC has not only the hydroxyl groups of the cellulose structure, but also carboxymethyl groups. The presence of different hydrophilic groups could have interesting implications on the cellular affinity of these structures compared to the referred previous work with microcrystalline cellulose.

Carboxymethyl cellulose is a polymer derived from cellulose. It has been introduced in tissue engineering to obtain composite scaffolds by combining it with substances like hydroxyapatite [12] or silk fibroin [13]. In that case, the authors demonstrated that carboxymethyl cellulose improves the biomineralization process because the carboxyl groups behave as nucleation sites for calcium ions. The effect of the introduction of carboxymethyl cellulose on the properties of the bulk materials of polycaprolactone-based composites was analyzed previously by the authors of the present work [14] although the manufacturing of 3D porous scaffolds made of these materials has not been reported before.

In this study, polycaprolactone–carboxymethyl cellulose (PCL:CMC) scaffolds have been manufactured by 3D printing and characterized in comparison with pure polycaprolactone ones in terms of morphology of the structures, mechanical properties and cell viability of the mesenchymal stem cells culture on their surfaces. Besides, an analysis of the flow behavior has been carried out in order to obtain a viscosity model useful for simulation and designing purposes.

The viscosity of the melt will affect the pressure drop in the melt flow channel. As this parameter is crucial to determine the power requirements to push the filament through the tip [15, 16], an optimal design of a device or a procedure to print structures by fused deposition modeling would require understanding the flow behavior of the material to be used. However, when a new material is proposed as an innovative feedstock of this type of manufacturing processes, this information is not usually offered by the authors. In this study, the viscosity isotherms at the operation temperature during 3D printing have been obtained.

## Materials and methods

### Material

Polycaprolactone (PCL) Capa<sup>®</sup> 6800 with mean molecular weight 80,000, melting point of 58–60 °C and melt flow index of 4.03–2.01 g/10 min was kindly supplied by Perstorp, carboxymethyl cellulose (CMC) with mean molecular weight 90,000 and a substitution degree of 0.7 carboxymethyl groups per anhydroglucose unit was purchased from Sigma Aldrich. Both polymeric materials were used as received. The following reagents were used for cell culture: DMEM low glucose (Sigma-Aldrich, UK), 100 units/ml

penicillin–streptomycin (P/S, Gibco, UK), PBS (Life Technologies), fetal calf serum-columbia (First Direct, First Link, UK), trypsin–EDTA (0.5%) (Thermo Fisher Scientific).

### Material compounding

PCL pellets were milled at 8000 rpm in an Ultra Centrifugal Mill ZM Retsch. This powder was mixed with the amount of CMC powder needed to obtain mixtures with 2% and 5% w/w content of carboxymethyl cellulose (named as PCL:CMC 98:2 and PCL:CMC 95:5, respectively). After homogenization, the mixture was subjected to compression molding with Collin P 200 P/M press. The cycle used consisted of a first step of heating at 20 °C/min up to 85 °C at constant pressure of 10 bar, keeping the temperature and the pressure for 2 min and subsequent cooling until room temperature at 20 °C/min. After this cycle, the sheet obtained was cut in small pellets that afterward were compressed and cut again in order to get homogeneous pellets of composite material.

### Flow properties

The viscosity of the polycaprolactone and its composites (PCL:CMC 98:2 and PCL:CMC 95:5) was evaluated in a rheometer built by the research group and validated in previous work [17]. This device consists of a main cylinder where the molten material goes through, an electrical resistance that heats the inside of the cylinder, PLC controller of the temperature, load cell, motor and CNC controller of the displacement. The nozzle of the cylinder is 0.30 mm diameter, and it has a  $L/D$  relation of 10.

Table 1 shows the temperature and extrusion rate values evaluated for each material. The temperature for this evaluation was 210 °C for PCL and PCL:CMC 98:2 and 200 °C for PCL:CMC 95:5. This temperature was chosen for the flow behavior analysis because the printing procedure was carried out at this value. On the other hand, preliminary trials of extrusion at 210 °C with PCL:CMC 95:5 failed because the residence time in the reservoir of material in the rheometer was excessive and the composite material became degraded. For this reason, the temperature analyzed for PCL:CMC 95:5 was 200 °C.

**Table 1** Temperature and extrusion rates used during the evaluation of the flow properties of PCL and its composites

Material	Temperature (°C)	Extrusion rates (mm/min)
PCL	210	4, 8, 30, 60, 90, 180
PCL:CMC 98:2	210	8, 30, 60, 90, 180
PCL:CMC 95:5	200	15, 30, 45, 60, 90, 180

During each extrusion trial, the evolution of the load applied was registered by a PCE-FG1k dynamometer. From this data, it is possible to calculate pressure and, therefore, apparent stress (Eq. 1).

$$\tau_{ap} = \frac{ROP}{2L} \quad (1)$$

where  $\tau_{ap}$  is apparent shear stress,  $R$  is radius of the capillary,  $OP$  is measured pressure drop,  $L$  is capillary length.

On the other hand, apparent shear rate can be calculated from volumetric data (Eq. 2).

$$\dot{\gamma}_{ap} = \frac{4Q}{\pi R^3} \quad (2)$$

where  $\dot{\gamma}_{ap}$  is apparent shear rate calculated assuming Newtonian behavior of the material,  $Q$  is volumetric flow.

Those values were used to determine the values of viscosity under the different conditions as described previously [17]. The data obtained were used to evaluate the dependence of the viscosity of the material with temperature and shear rate. These data were fitted to the power law equation (Eq. 3) in order to analyze the nature of the materials (shear-thinning or shear-thickening) and if the presence of the carboxymethyl cellulose modifies, the flow behavior of the polycaprolactone matrix:

$$\eta = K \cdot \dot{\gamma}^{n-1} \quad (3)$$

where  $\eta$  is the viscosity of the material,  $K$  is the consistency index of the power law equation,  $\dot{\gamma}$  is the calculated shear rate, and  $n$  is the power law index.

The power-law model is the equation that is normally used to analyze the behavior of the feed material in fused deposition modeling liquefiers [16]. This is the reason why this mathematical expression has been chosen in the present study.

## Scaffolds manufacturing

Prior to print the scaffolds, it was necessary to manufacture the filaments to be fed to the 3D printer. For this purpose, PCL, PCL:CMC 98:2 and PCL:CMC 95:5 pellets were fed into an extruder to obtain a continuous filament useful as feedstock for fused deposition modeling. This lab-extruder was formed by a feeding chute, a stepper motor and mechanical transmission, an electrical resistance, a 8 mm screw and cylinder with a  $L/D$  relationship of 10 and a nozzle tip of 1,5 mm. After extrusion, the filament was cooled with water to get a constant diameter. The temperature used was 120 °C and the rotating speed, 7 rpm.

The scaffolds were obtained by additive manufacturing in a commercial device (Prusa i3) with a 0.4 mm nozzle tip. The

pattern of the structure was 0°–90°, and the height between layers was settled at 0.3 mm. The 0°–90° provides square and interconnected pores which have been demonstrated to provide improved mechanical properties (compared to other possible arrangements) [18] and ensure the vascularization of the scaffold.

The parameters were set on 210 °C and 25 mm/s. During the determination of the flow properties of the composite materials, 210 °C was stated as an excessive value of the temperature for the processing of PCL:CMC 95:5 because of its degradation. However, as the residence time was significantly lower in the commercial 3D printer, the temperature of 210 °C is suitable because the reduced viscosity prevents the clogging of the nozzle. The reduced residence time in the 3D printer can be deeply understood with the model proposed by Osswald et al. [19], who discussed that the molten material in the liquefier chamber of a fused deposition modeling 3D printer is a thin layer above the nozzle tip, so the material is in the molten state for a short period of time. Therefore, the degradation of the material because of an extended time at high temperature in the molten state can be avoided.

The three materials were processed under the same operating conditions in order to ensure that the differences observed during the study are caused by the change of material and not by the change on the processing parameters, as the parameters have significant influence on the mechanical properties and morphology of the parts [20].

## Morphology

The morphology of the scaffolds was evaluated by optical and electron microscopy. Scanning electron microscopy (SEM) was conducted on a TM3030 Hitachi device at an acceleration voltage of 15 kV.

The distance between struts was measured ( $\approx 50$ ) with the software of the optical microscope Olympus BX51. This distance can be identified as the pore size because of the square shape of the pores due to the 0°–90° pattern used during the manufacturing.

The porosity of the structures was assessed by using the following equation (Eq. 4) [21, 22]:

$$\% \text{ porosity} = 100 \left( 1 - \frac{\rho_{ap}}{\rho_{bulk}} \right) \quad (4)$$

In this Eq. 4,  $\rho_{ap}$  is the apparent density of the scaffold. This parameter was calculated by the ratio between the mass of the sample and its volume ( $n = 6$ ). On the other hand,  $\rho_{bulk}$  is the density of the bulk material. The measurement of  $\rho_{bulk}$  was carried out by measuring the mass and the volume of short filaments ( $n = 8$ ). For both cases, the dimensions were measured with a caliper ( $\pm 0.01$  mm).

## Mechanical testing

Polycaprolactone has been widely studied for bone tissue engineering. Long bones behave better under compression loads than under other types of loads [23]. Therefore, it is common to study preferably the compression characteristics of a material expected to be used for bone replacement [22, 24, 25].

In this study, four replicas of scaffolds of  $8 \times 4 \times 4 \text{ mm}^3$  (height  $\times$  length  $\times$  width) were subjected to static compression characterization. The compression tests were made in a universal test machine Zwick Roell Z0.5 at crosshead speed of 1 mm/min. The compression modulus was calculated using the first part of the linear segment of the stress–strain curve and the initial cross-sectional area. The strain ( $\sigma$ ) was calculated as the ratio between the force measured ( $F$ ) and the apparent cross section of the scaffold ( $A$ ) (Eq. 5).

$$\sigma = F/A \quad (5)$$

Strain ( $\epsilon$ ) was defined as the ratio between the difference of height at each point ( $Oh$ ) and the initial height of the scaffold ( $h_0$ ) (Eq. 6).

$$\epsilon = Oh/h_0 \quad (6)$$

On the other hand, the stress at yield was assessed as the first point on the stress–strain curve where an increase in strain occurs without an increase in stress, according to the definition established in the standard ASTM D1621-16.

## Cell culture

Bone marrow mesenchymal stem cells of passage 2 were used to evaluate the bioactivity of the PCL:CMC 98:2 and PCL scaffolds developed in this work. Bone marrow aspirates of 5 ml were obtained from sheep ( $n=1$ ) and placed in heparinized tube. The aspirate was then transferred to a T225 cell culture flask (Corning, Thermo Fisher Scientific UK) prefilled with low glucose Dulbecco's Modified Eagle Medium (DMEM) (Sigma-Aldrich, Dorset, UK) supplemented with 1% penicillin–streptomycin (10,000 U/ml) and 10% fetal calf serum. After 3 days, the cells were washed with PBS and fresh culture media was added to the flask. Once cells were 80–90% confluent, they were trypsinized, counted and re-plated with culture medium that was changed every 2 days.

Three replicas for each group of samples (PCL and PCL:CMC 98:2) were cut with a scalpel. These samples were square in shape with an area of  $16 \text{ mm}^2$  and a thickness of 8 mm. The samples were measured with a caliper to ensure that the volume of the replicas was the same. PCL:CMC 95:5 samples were not used for biological evaluation as their

mechanical properties are significantly worse than pure PCL samples. This point will be further explained in the Results and Discussion section.

Prior to seeding, samples were cleaned in distilled water, followed by further washing twice with PBS, twice with ethanol and then again twice with PBS in order to remove any trace of ethanol from the samples. Every cleaning step lasted 15 min. All the cleaning processes took place under the hood after ethanol immersion to avoid infection. Once this procedure was finished, the parts were placed in non-treated well plates and sterilized under UV light for 12 h.

A dynamic seeding technique was used to culture the cells on the scaffolds. A 1 ml suspension of 150,000 cells was introduced to the tubes containing the scaffolds. The tubes were stirred with a tube rotator (MACSmix, Miltenyi Biotec) at 12 rpm for 1 h in the incubator at  $37^\circ\text{C}$  and 5%  $\text{CO}_2$ . Then, 7 ml of fresh media were added and the tubes were left in the incubator until reaching the required time points (1, 3, 6, 8 and 10 days).

## Viability tests

The cell viability was studied at days 1, 3, 6 and 8 of culture by Alamar Blue<sup>®</sup> assay (Thermo fisher scientific, UK). At each time point, the culture media was removed and scaffolds were washed with PBS and transferred to new tubes. Then, fresh culture media with 10% (v/v) Alamar blue in DMEM were added. The samples were incubated with the reagent for 4 h at  $37^\circ\text{C}$ . After the incubation time, reaction product of the samples and controls were measured in duplicates of 100  $\mu\text{l}$  at fluorescence excitation wavelength of 540 nm and an emission wavelength of 590 nm in a microplate reader (Tecan, Infinite Pro 200 series, Switzerland). Samples consisting of the Alamar Blue reagent solution without cells were used as negative controls of the described protocol.

## Statistical analysis

For every quantitative characterization procedure, the Wilcoxon test [26] was used to determine if the results from every group of samples show a significant difference compared to pure PCL results ( $p < 0.05$  for significant,  $p < 0.01$  for highly significant,  $p < 0.001$  for very highly significant statistical difference). The implementation of the Wilcoxon test was carried out with MATLAB 7.4. (2007) software (MathWorks). All the figures show the mean values of each group, and their standard deviation is represented with error bars.

**Table 2** Parameters of the viscosity isotherms for pure polycaprolactone and its composites

Material	Temperature (°C)	Power law index	Consistency index (Pa s <sup>2</sup> )	Adjusted R <sup>2</sup>
PCL	210	0.379	18,163	0.9977
PCL:CMC 98:2	210	0.314	37,053	0.9958
PCL:CMC 95:5	200	0.272	54,796	0.9959

## Results and discussion

### Flow properties

Table 2 shows the values of the characteristic values of the parameters of the power-law equation. The power law index is  $< 1$ , and the materials can be classified as pseudoplastic (also called shear-thinning) materials. The shear-thinning effect occurs when the shear stress disentangles the macromolecular chains and they become oriented to the flow direction. This orientation enhances the flow of the melt and, as a consequence, its viscosity is reduced. This behavior is typical of polymeric fluids and melts [15].

The values of the consistency index ( $K$ ) are a measure of the viscosity of the fluid, while the power law index ( $n$ ) is an indicative of the flow behavior of the material [27]. According to the values presented in Table 2,  $K$  values are higher for the PCL:CMC blends than for PCL alone and, hence, the blend has higher values of viscosity. This increment of the viscosity is caused by the presence of the CMC particles that difficulties the flow of the molten material. This effect has already been reported for the introduction of particulate agricultural waste used as biofillers in a polycaprolactone matrix [28]. This increase in the viscosity due to the introduction of the filler explains why the operation temperature needs to be increased for the 3D printing of the composite materials, compared to the reported values for pure PCL scaffolds [2, 22].

On the other hand, the power law index values are in the common range referred for polymeric systems and particulate slurries [27]. The lower values of the power law index for the PCL:CMC composite materials involves a higher reduction of the viscosity for high shear rates values. Kalambur and Rizvi [29] reported a similar increment of the consistency index in polycaprolactone matrices with starch.

### Morphology

The scaffolds made of PCL, PCL:CMC 98:2 and PCL:CMC 95:5 show a well-defined internal geometry with interconnected pores (Fig. 1), showing the typical mesostructured of conventional polymers, well known in fused deposition modeling, such as ABS or PLA.

The SEM observation of the composite parts (Fig. 2) allows a clearer observation of the surface of the structures. In these images, it is possible to see that the parts containing 5% w/w of carboxymethyl cellulose have a rough surface with the presence of elongated micropores on the filaments. The presence of these micropores can be explained because of a worse deposition process due to the presence of agglomerates of particles, as they hinder the extrusion process. A high concentration of the additive enhances the formation of agglomerates, as demonstrated in the characterization of these composites in the bulk form [14]. Therefore, according to the observations in Fig. 2, it is possible to confirm that 5% w/w is an excessive concentration of carboxymethyl cellulose to obtain a smooth surface of the filaments obtained by fused deposition modeling with the procedure proposed in the present study. Canti et al. [30] referred in their work a similar trend in their composite materials (ABS-based): above a maximum value of the concentration of the filler the printability of the material is hindered and, therefore, it is not possible to obtain suitable 3D-printed parts with these composites.

All the results related to the analysis of the porosity of the 3D-printed structures are shown in Table 3. The apparent density for all the groups of scaffolds analyzed in this work is between 0.52 and 0.56 g/cm<sup>3</sup>, values within the range reported for spongy bone [31] (0.14–1.2 g/cm<sup>3</sup>). Something similar can be confirmed for the porosity values, which are between 50 and 54%. They are similar to other reported values for scaffolds to be used for bone regeneration [22, 32]. In this case, it is possible to highlight that the higher values of porosity have been found for PCL:CMC 95:5 due to the presence of the micropores shown in Fig. 2. Finally, the pore size suitable for bone regeneration has been established between 150 and 500  $\mu\text{m}$  [33, 34], and an improved osteogenesis is achieved with a pore size above 300  $\mu\text{m}$  [8]. All the groups of scaffolds also fulfill this requirement, as the pore size (evaluated as the distance between struts) was found to be between 420 and 465  $\mu\text{m}$ . Besides, it is important to notice that the deviation is less of 10%, which is a reference of the regularity of the pore size of the parts obtained.

### Mechanical testing

As shown in Table 4, the carboxymethyl cellulose loading has a negative effect on the mechanical properties of the com-



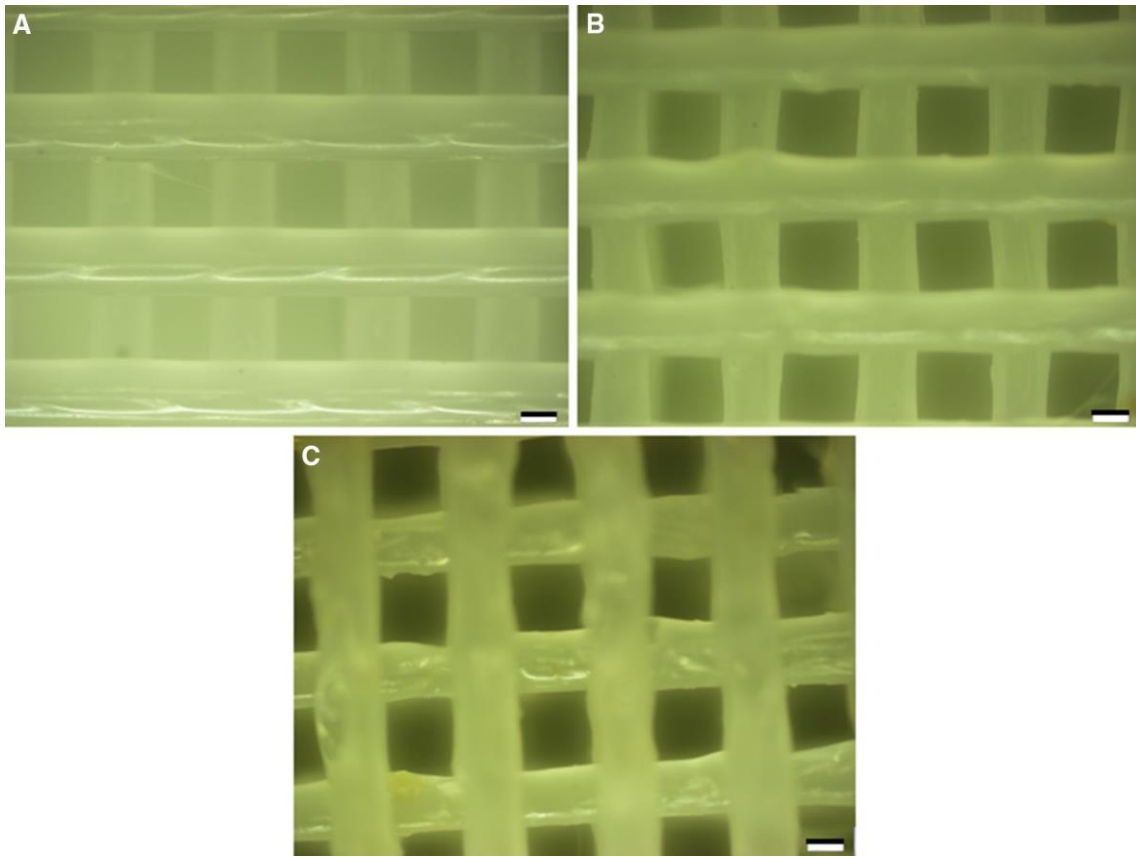


**Fig. 1** Pictures from optical microscope of the structure of PCL (a), PCL:CMC 98:2 (b) and PCL:CMC 95:5 (c) structures (scale bar: 200  $\mu\text{m}$ )

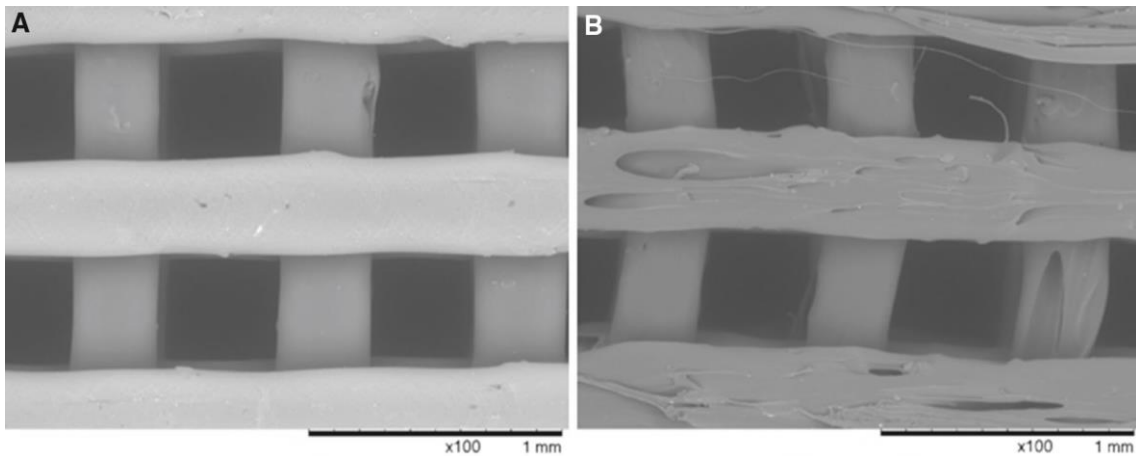


**Fig. 2** SEM pictures of PCL:CMC 98:2 (a) and PCL:CMC 95:5 (b) structures (scale bar: 1 mm)

posite scaffolds, as the compression modulus decreases when the concentration of the additive is increased. This reduction is not statistically significant ( $p > 0.05$ ) for PCL:CMC 98:2 samples, but it is significant ( $p < 0.05$ ) for PCL:CMC 95:5 compared to the value for pure PCL scaffolds.

Also in Table 4, the values of the compression modulus reported from other authors for similar structures have been included with comparative purposes. The data obtained in

this work for PCL scaffolds and those reported in the literature [7, 23] are close to the lower limit of the range of the compressive modulus of cancellous bone [8]. However, composite scaffolds containing 5% CMC have a significantly lower compression modulus. For this reason, this combination was not subjected to the *in vitro* biological evaluation, as the mechanical similarity to the surrounding tissue is a key

**Table 3** Apparent density, porosity and distance between struts of polycaprolactone and composite structures

Material	Apparent density (g/cm <sup>3</sup> )	Porosity (%)	Distance between struts (μm)
PCL	0.52 ± 0.03	52.3 ± 2.5	463 ± 26
PCL:CMC 98:2	0.56 ± 0.02*	50.6 ± 2.0	462 ± 45*
PCL:CMC 95:5	0.53 ± 0.02	53.1 ± 1.8	422 ± 35***

\* $p < 0.05$ ; \*\*\* $p < 0.001$  compared to the group of pure PCL samples

**Table 4** Compression modulus of the structures proposed in this work and the similar ones analyzed in the state of art

Structure	Compression modulus	Reference
PCL 3D printed parts	25.2 ± 3.3	This work
PCL:CMC 98:2 printed parts	18.7 ± 3.1	This work
PCL:CMC 95:5 printed parts	12.5 ± 4.0*	This work
Cancellous bone	20–500 MPa	[8]
PCL 3D printed parts	34.2 MPa	[22]
PCL	42.2	[7]
PCL/CaP (coated)	41.9	[7]
PCL/50-45S5	36.4	[7]

aspect for a suitable in vivo performance of scaffolds to be used in Bone Tissue Engineering applications.

Regarding the values of the stress at yield, the mean values are  $2.08 \pm 0.18$  MPa for PCL,  $2.12 \pm 0.15$  MPa for PCL:CMC 98:2 and  $2.35 \pm 0.51$  MPa for PCL:CMC 95:5, with no significant difference ( $p > 0.05$ ) between the groups of data. Therefore, contrary to the effect of microcrystalline cellulose on the 3D-printed structures made of microcrystalline cellulose–polycaprolactone composites [11], carboxymethyl cellulose does not have a reinforcement effect. This lack of reinforcement can be explained by the presence of the micropores observed by SEM observation in Fig. 2. These micropores affect the layer–layer adhesion and, therefore, the mechanical integrity of the structure is weakened.

### Viability tests

Figure 3 shows the results of the viability test carried out on the PCL and PCL:CMC 98:2 samples. At Day 1, viability is significantly higher ( $p < 0.05$ ) on PCL:CMC 98:2 samples compared to PCL. This may be due to the increased attachment of cells on the composite scaffold compared to PCL. The comparison of these results to the previous work on PCL:CMC samples in the bulk form [14] confirm that the

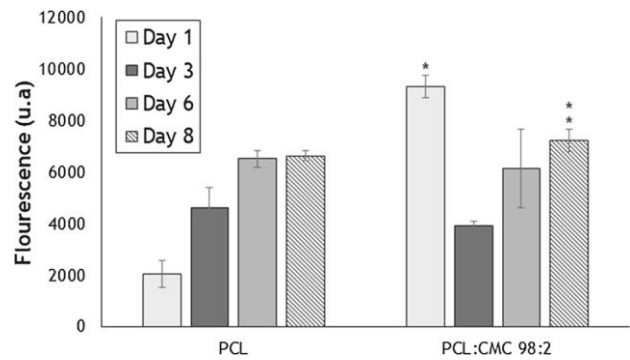


**Fig. 3** Viability test results for 3D printed polycaprolactone and PCL:CMC 98:2 samples (\* $p < 0.05$ ; \*\* $p < 0.01$  compared to pure PCL samples)

structure of the samples plays an essential role on the promotion of cell attachment. In that case, no difference was observed between the pure polycaprolactone samples and the composite ones. This difference can be explained by the increased surface area on 3D-printed samples. An increased surface offers the cells higher probability to find points with high carboxymethyl cellulose content which can improve the cell adhesion processes.

However, at Day 3 a decrease in the fluorescence value was observed. After this drop, cells were able to recover. In fact, there is a clear improvement on the viability between Day 6 and Day 8. Between these two time points, the cells on polycaprolactone scaffolds reached their plateau, while the cells on composite scaffolds are able to provide an increase in their fluorescence value from the Alamar Blue<sup>®</sup> assay.

The increase on the cell viability for the composite samples can be explained by the increased hydrophilicity of the PCL:CMC 98:2 compared to pure polycaprolactone, which may have resulted in higher cell attachment and proliferation [14]. However, as the cell adhesion and spreading processes depend on many factors [35], other parameters could be also responsible for this improvement, such as topography changes due to differences on the surface of the filaments because of the presence of the particles.

### Conclusions

Carboxymethyl cellulose–polycaprolactone scaffolds were obtained by 3D printing techniques. The structures manufactured have regular and controlled porosity which fulfills the requirements described in the literature for scaffolds to be used in bone regeneration. Nevertheless, the introduction of the additive worsens the compression properties of the scaffolds. This reduction is significant ( $p < 0.05$ ) for the samples containing 5% w/w of carboxymethyl cellulose but it is not for the samples containing 2% w/w, so these last ones

can still be taken into consideration for their application for bone regeneration. Furthermore, the samples containing 2% w/w of carboxymethyl cellulose improve stem cells proliferation, as shown in the viability tests carried out during this study. Therefore, the polycaprolactone–carboxymethyl cellulose scaffolds have interesting properties for their further analysis as support material in bone tissue engineering.

In addition to this, in this study flow behavior modeling has been carried out. The expressions obtained could be useful in order to simulate and design new processes for polycaprolactone and polycaprolactone composites.

**Acknowledgements** M.E. Alemán-Domínguez would like to express her gratitude for the funding through the PhD Grant Program of Las Palmas de Gran Canaria University (Code of the Grant: PIFULPGC-2014-ING-ARQU-2). The authors would like to thank H2020-MSCA-RISE program, as this work is part of developments carried out in BAMOS project, funded from the European Union’s Horizon 2020 research and innovation programme under Grant Agreement No. 734156.

## References

- Mondal D, Griffith M, Venkatraman SS (2016) Polycaprolactone-based biomaterials for tissue engineering and drug delivery: current scenario and challenges. *Int J Polym Mater Poym Biomater* 65(5):255–265. <https://doi.org/10.1080/00914037.2015.1103241>
- Hutmacher DW, Schantz T, Zein I, Ng KW, Teoh SH, Tan KC (2001) Mechanical properties and cell cultural response of polycaprolactone scaffolds designed and fabricated via fused deposition modeling. *J Biomed Mater Res* 55(2):203–216
- Jiang W, Shi J, Li W, Sun K (2012) Morphology, wettability, and mechanical properties of polycaprolactone/hydroxyapatite composite scaffolds with interconnected pore structures fabricated by a mini-deposition system. *Polym Eng Sci* 52(11):2396–2402. <https://doi.org/10.1002/pen.23193>
- Cai Y, Li J, Poh CK, Tan HC, San Thian E, Hsi Fuh JY, Sun J, Tay BY, Wang W (2013) Collagen grafted 3D polycaprolactone scaffolds for enhanced cartilage regeneration. *J Mater Chem B* 1(43):5971–5976. <https://doi.org/10.1039/c3tb20680g>
- Mirhosseini MM, Haddadi-Asl V, Zargarian SS (2016) Fabrication and characterization of hydrophilic poly( $\epsilon$ -caprolactone)/pluronic P123 electrospun fibers. *J Appl Polym Sci*. <https://doi.org/10.1002/app.43345>
- Mehr NG, Li X, Chen G, Favis BD, Hoemann CD (2015) Pore size and LbL chitosan coating influence mesenchymal stem cell in vitro fibrosis and biomineralization in 3D porous poly( $\epsilon$ -caprolactone) scaffolds. *J Biomed Mater Res A* 103(7):2449–2459. <https://doi.org/10.1002/jbm.a.35381>
- Poh PSP, Hutmacher DW, Holzapfel BM, Solanki AK, Stevens MM, Woodruff MA (2016) In vitro and in vivo bone formation potential of surface calcium phosphate-coated polycaprolactone and polycaprolactone/bioactive glass composite scaffolds. *Acta Biomater* 30:319–333. <https://doi.org/10.1016/j.actbio.2015.11.012>
- Dávila JL, Freitas MS, Inforçatti Neto P, Silveira ZC, Silva JVL, D’Ávila MA (2016) Fabrication of PCL/ $\beta$ -TCP scaffolds by 3D mini-screw extrusion printing. *J Appl Polym Sci*. <https://doi.org/10.1002/app.43031>
- Arafat MT, Lam CXF, Ekaputra AK, Wong SY, Li X, Gibson I (2011) Biomimetic composite coating on rapid prototyped scaffolds for bone tissue engineering. *Acta Biomater* 7(2):809–820. <https://doi.org/10.1016/j.actbio.2010.09.010>
- Rodríguez G, Dias J, D’Ávila MA, Bártolo P (2013) Influence of hydroxyapatite on extruded 3D scaffolds. In: *Procedia Engineering*. pp 263–269. <https://doi.org/10.1016/j.proeng.2013.05.120>
- Alemán-Domínguez ME, Giusto E, Ortega Z, Tamaddon M, Benítez AN, Liu C (2018) Three-dimensional printed polycaprolactone–microcrystalline cellulose scaffolds. *J Biomed Mater Res B*. <https://doi.org/10.1002/jbm.b.34142>
- Pasqui D, Torricelli P, De Cagna M, Fini M, Barbucci R (2014) Carboxymethyl cellulose–hydroxyapatite hybrid hydrogel as a composite material for bone tissue engineering applications. *J Biomed Mater Res A* 102(5):1568–1579. <https://doi.org/10.1002/jbm.a.34810>
- Singh BN, Panda NN, Mund R, Pramanik K (2016) Carboxymethyl cellulose enables silk fibroin nanofibrous scaffold with enhanced biomimetic potential for bone tissue engineering application. *Carbohydr Polym* 151:335–347. <https://doi.org/10.1016/j.carbpol.2016.05.088>
- Alemán-Domínguez ME, Ortega Z, Benítez AN, Vilariño-Feltrer G, Gómez-Tejedor JA, Vallés-Lluch A (2018) Tunability of polycaprolactone hydrophilicity by carboxymethyl cellulose loading. *J Appl Polym Sci*. <https://doi.org/10.1002/app.46134>
- Ramanath HS, Chua CK, Leong KF, Shah KD (2008) Melt flow behaviour of poly- $\epsilon$ -caprolactone in fused deposition modelling. *J Mater Sci Mater M* 19(7):2541–2550. <https://doi.org/10.1007/s10856-007-3203-6>
- Turner BN, Strong R, Gold SA (2014) A review of melt extrusion additive manufacturing processes: I. Process design and modeling. *Rapid Prototyp J* 20(3):192–204. <https://doi.org/10.1108/rpj-01-2013-0012>
- Ortega Z, Alemán ME, Benítez AN, Monzón MD (2016) Theoretical-experimental evaluation of different biomaterials for parts obtaining by fused deposition modeling. *Measurement* 89:137–144. <https://doi.org/10.1016/j.measurement.2016.03.061>
- Moroni L, De Wijn JR, Van Blitterswijk CA (2006) 3D fiber-deposited scaffolds for tissue engineering: influence of pores geometry and architecture on dynamic mechanical properties. *Biomaterials* 27(7):974–985. <https://doi.org/10.1016/j.biomaterials.2005.07.023>
- Osswald TA, Puentes J, Kattinger J (2018) Fused filament fabrication melting model. *Addit Manuf* 22:51–59. <https://doi.org/10.1016/j.addma.2018.04.030>
- Abbott AC, Tandon GP, Bradford RL, Koerner H, Baur JW (2016) Process parameter effects on bond strength in fused filament fabrication. In: *International SAMPE technical conference*
- Yang GH, Kim M, Kim G (2017) Additive-manufactured polycaprolactone scaffold consisting of innovatively designed micro-sized spiral struts for hard tissue regeneration. *Biofabrication*. <https://doi.org/10.1088/1758-5090/9/1/015005>
- Domingos M, Intranuovo F, Gloria A, Gristina R, Ambrosio L, Bártolo PJ, Favia P (2013) Improved osteoblast cell affinity on plasma-modified 3-D extruded PCL scaffolds. *Acta Biomater* 9(4):5997–6005. <https://doi.org/10.1016/j.actbio.2012.12.031>
- Ward R (1990) *Foundations of osteopathic medicine*. Lippincott Williams and Wilkins, Illinois
- Farzadi A, Waran V, Solati-Hashjin M, Rahman ZAA, Asadi M, Osman NAA (2015) Effect of layer printing delay on mechanical properties and dimensional accuracy of 3D printed porous prototypes in bone tissue engineering. *Ceram Int* 41(7):8320–8330. <https://doi.org/10.1016/j.ceramint.2015.03.004>
- Naghieh S, Karamooz Ravari MR, Badrossamay M, Foroosmeh E, Kadkhodaei M (2016) Numerical investigation of the mechanical properties of the additive manufactured bone scaffolds fabricated by FDM: the effect of layer penetration and post-heating. *J Mech*



- 
- Behav Biomed 59:241–250. <https://doi.org/10.1016/j.jmbbm.2016.01.031>
26. Motulsky H (2016) Essential biostatistics. A nonmathematical approach. Oxford University Press, New York
  27. Chandra A, Chhabra RP (2011) Influence of power-law index on transitional Reynolds numbers for flow over a semi-circular cylinder. *Appl Math Model* 35(12):5766–5785. <https://doi.org/10.1016/j.apm.2011.05.004>
  28. Hejna A, Formela K, Saeb MR (2015) Processing, mechanical and thermal behavior assessments of polycaprolactone/agricultural wastes biocomposites. *Ind Crop Prod* 76:725–733. <https://doi.org/10.1016/j.indcrop.2015.07.049>
  29. Kalambur S, Rizvi SSH (2006) Rheological behavior of starch–polycaprolactone (PCL) nanocomposite melts synthesized by reactive extrusion. *Polym Eng Sci* 46(5):650–658. <https://doi.org/10.1002/pen.20508>
  30. Canti E, Aydın M (2018) Effects of micro particle reinforcement on mechanical properties of 3D printed parts. *Rapid Prototyp J* 24(1):171–176. <https://doi.org/10.1108/rpj-06-2016-0095>
  31. Fayyazbakhsh F, Solati-Hashjin M, Keshtkar A, Shokrgozar MA, Dehghan MM, Larijani B (2017) Novel layered double hydroxides–hydroxyapatite/gelatin bone tissue engineering scaffolds: fabrication, characterization, and in vivo study. *Mater Sci Eng C* 76:701–714. <https://doi.org/10.1016/j.msec.2017.02.172>
  32. Ostrowska B, Di Luca A, Moroni L, Swieszkowski W (2016) Influence of internal pore architecture on biological and mechanical properties of three-dimensional fiber deposited scaffolds for bone regeneration. *J Biomed Mater Res A* 104(4):991–1001. <https://doi.org/10.1002/jbm.a.35637>
  33. Chuenjitkuntaworn B, Inrung W, Damrongsri D, Mekaapiruk K, Supaphol P, Pavasant P (2010) Polycaprolactone/hydroxyapatite composite scaffolds: preparation, characterization, and in vitro and in vivo biological responses of human primary bone cells. *J Biomed Mater Res A* 94(1):241–251. <https://doi.org/10.1002/jbm.a.32657>
  34. Gómez-Lizárraga KK, Flores-Morales C, Del Prado-Audelo ML, Álvarez-Pérez MA, Piña-Barba MC, Escobedo C (2017) Polycaprolactone- and polycaprolactone/ceramic-based 3D-bioprinted porous scaffolds for bone regeneration: a comparative study. *Mater Sci Eng C Mater* 79(Supplement C):326–335. <https://doi.org/10.1016/j.msec.2017.05.003>
  35. Chen S, Guo Y, Liu R, Wu S, Fang J, Huang B, Li Z, Chen Z (2018) Tuning surface properties of bone biomaterials to manipulate osteoblastic cell adhesion and the signaling pathways for the enhancement of early osseointegration. *Colloid Surf B* 164:58–69. <https://doi.org/10.1016/j.colsurfb.2018.01.022>